In-Cell NMR Spectroscopy

Deutsche Ausgabe: DOI: 10.1002/ange.201601850
Internationale Ausgabe: DOI: 10.1002/anie.201601850

Studying Intrinsically Disordered Proteins under True In Vivo Conditions by Combined Cross-Polarization and Carbonyl-Detection NMR Spectroscopy

Juan Lopez, Robert Schneider, Francois-Xavier Cantrelle, Isabelle Huvent, and Guy Lippens**

Abstract: *Under physiological conditions, studies of intrinsically disordered proteins (IDPs) by conventional NMR methods based on proton detection are severely limited by fast amide-proton exchange with water. ^{13}C detection has been proposed as a solution to the exchange problem, but is hampered by low sensitivity. We propose a new pulse sequence combining proton–nitrogen cross-polarization and carbonyl detection to record high-resolution, high-sensitivity NMR spectra of IDPs under physiological conditions. To demonstrate the efficacy of this approach, we recorded a high-quality N–CO correlation spectrum of α-synuclein in bacterial cells at 37°C.*

Protein structure and dynamics are strongly dependent on solvent and temperature, thus making studies under true physiological conditions important for understanding the biological behavior of proteins. In-cell NMR spectroscopy has thus become an important tool for gaining an understanding of biomolecular mechanisms.[1–6] Recent progress in NMR spectroscopy, including the exploitation of amide-proton and water magnetization under conditions under which only the amide protons are excited, as well as direct carbon-atom detection, has made it possible record NMR spectra of biomolecules under near-physiological conditions of temperature and pH value.[7] At around the same time, Yuwen and Skrynnikov[8] showed that the initial INEPT transfer in a standard $^{1}H,^{15}N$ HSQC pulse sequence could be advantageously replaced by a J-cross-polarization (J-CP) transfer,[9–12] since this excitation mechanism uses the large water-magnetization reservoir to continuously replenish the amide-proton magnetization.[8] Herein, we describe the combination of both approaches—J-CP excitation and CO detection—and present an improved NMR experiment that enables an N-CO spectrum to be recorded under truly mammalian physiological conditions, that is, at 37°C and pH 7.4. We optimized the experiment in vitro on α-synuclein, an intrinsically disordered protein involved in Parkinson's disease and obtained a high-resolution N-CO spectrum of α-synuclein in bacterial cells at 37°C.

Comparison of different $^{1}H,^{15}N$ spectra (sensitivity-enhanced HSQC[13] or BEST-HSQC[14]) shows that fast amide-proton exchange with water (as expected for α-synuclein at pH 7.4 and 37°C; see Table S1 in the Supporting Information) during the H–N polarization-transfer step in a classical INEPT transfer and during the subsequent ^{15}N evolution destroys antiphase H–N coherence and leads to serious loss of intensity or even complete disappearance of the majority of signals under these physiological conditions (see Figure S1 in the Supporting Information). The signal loss during the initial transfer step can be minimized by the use of a J-CP polarization-transfer scheme rather than the classical INEPT transfer.[8] J-CP transfer outperforms J-coupling-based INEPT as it pumps water magnetization to the amide nitrogen atom, but provides only a marginal advantage in the reverse nitrogen–proton polarization transfer.[8] Additionally, nitrogen in-phase evolution under proton decoupling prevents intensity loss through solvent exchange during the indirect evolution.[15,16] An initial J-CP transfer combined with proton decoupling during nitrogen evolution and INEPT back transfer gives the CP-HISQC sequence[8] with improved performance under conditions of fast exchange (see Figure S2). For rapidly exchanging amide functionalities, the CP-HISQC experiment performs better, whereas for residues with amide protons in slow exchange, peak intensity is still higher with other sequences, such as BEST or sensitivity-enhanced HSQC (see Figure S2). For α-synuclein under physiological conditions, magnetization loss during the back transfer is severe for most residues in all types of HSQC spectra (see Figure S1).

Avoiding back-transfer from the amide nitrogen atom to the proton by direct carbonyl observation leads to N–CO correlation spectra[18–23] with even better spectral dispersion.[24] When implemented by starting directly from ^{13}C magnetization, however, the experiment suffers from lower sensitivity, which has motivated the implementation of modified ^{13}CO pulse sequences that start from proton magnetization.[25,26] The BEST-H_NNCO sequence further involves the selective excitation of only the amide protons to enhance the rapid longitudinal relaxation of the amide term by water exchange.[7] This sequence gives excellent

[*] Dr. J. Lopez, Dr. R. Schneider, Dr. F.-X. Cantrelle, Dr. I. Huvent, Dr. G. Lippens
Université de Lille, CNRS, UMR 8576
UGSF—Unité de Glycobiologie Structurale et Fonctionnelle
59000 Lille (France)
E-mail: juan.lopez@pucp.edu.pe
Dr. J. Lopez
Departamento de Ciencias-Quimica
Pontificia Universidad Catolica del Peru
Av. Universitaria 1801, Lima 32 (Peru)
Dr. G. Lippens
Laboratoire d'Ingénierie des Systèmes Biologiques et des Procédés
Université de Toulouse, CNRS, INRA, INSA Toulouse
135 Avenue de Rangueil, 31077 Toulouse (France)
E-mail: glippens@insa-toulouse.fr
Supporting information and the ORCID identification number(s) for the author(s) of this article can be found under http://dx.doi.org/10.1002/anie.201601850.

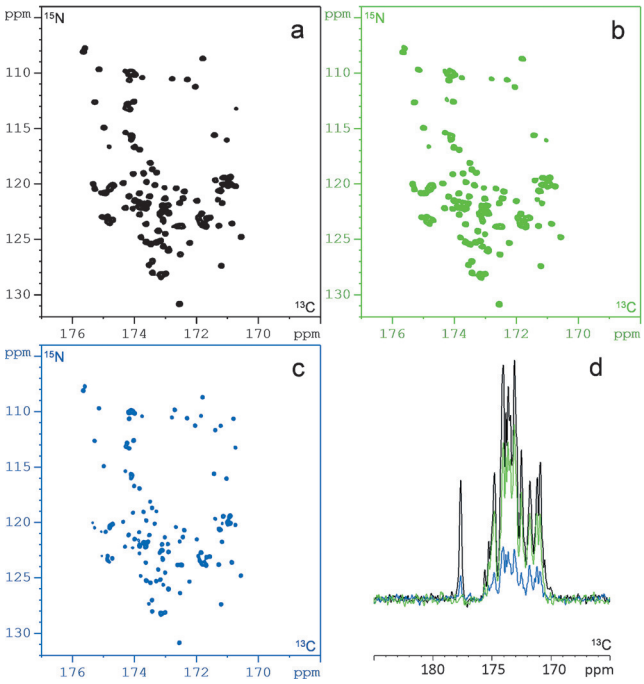

Figure 1. a) CP-H_NNCO, b) BEST-H_NNCO, and c) CON spectra of α-synuclein in vitro at 10 °C. d) Superposition of the first increments of the CP-H_NNCO (black), BEST-H_NNCO (green), and CON spectra (blue). The α-synuclein sample was produced and purified as described previously.[17] For experimental conditions, see the Supporting Information.

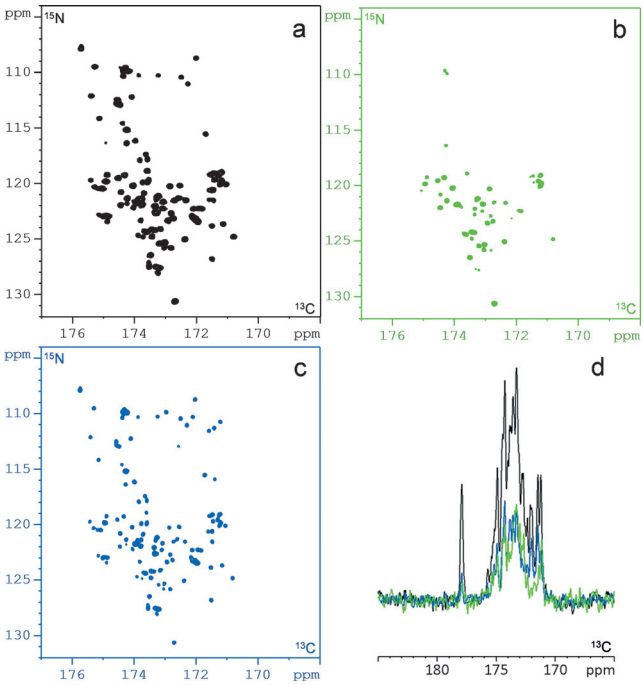

Figure 2. a) CP-H_NNCO, b) BEST-H_NNCO, and c) CON spectra of α-synuclein in vitro at 37 °C. d) Superposition of the first increments of the CP-H_NNCO (black), BEST-H_NNCO (green), and CON spectra (blue). For experimental conditions, see the Supporting Information.

results at low temperatures (Figure 1), and spectra under near-physiological conditions have been reported.[7] However, when we recorded spectra of α-synuclein under truly physiological conditions of 37 °C and pH 7.4, even this optimized pulse sequence suffered from significant signal loss, whereby rapidly exchanging peaks had an even lower signal-to-noise ratio than the same peaks in the direct carbon-excitation CON spectrum (Figures 2, 4).

We propose to combine the advantages of both J-CP transfer and CO direct detection by using an initial transfer of magnetization from the amide proton to its attached nitrogen atom through J-CP, ^{15}N t_1 evolution under continuous proton decoupling, and subsequent transfer of the ^{15}N term to the carbonyl atom of the preceding residue through classical INEPT (Figure 3). Carbonyl groups are detected by virtual decoupling, by combining the in-phase and antiphase (IP/AP) signals after shifting both lines.[19] Of special interest is the water magnetization, as it constitutes the main mechanism for replenishment of the amide-proton vector after the recycling delay. During the initial CP transfer, water magnetization is locked along the x axis by the (off-resonance) proton DIPSI2 pulse train, and then stored along the z axis by a hard 90° pulse (ϕ2, Figure 3). As in the original study, we used a field strength of 4 kHz for the DIPSI2 CP on both channels, but optimized the duration for each temperature. As the total DIPSI2 cycle[27,28] takes 7.2 ms, we relaxed the condition of using only half-integer multiples of the cycle, and implemented the pulse sequence in such a way the CP transfer could be stopped at n/4 multiples of the total DIPSI2 cycle. Optimization of the CP transfer (see Figure S3) yielded values of $t_m = 7/4 \times t_{DIPSI2} = 12.6$ ms at 10 and 20 °C, $t_m = 9/4 \times t_{DIPSI2} = 16.2$ ms at 30 and 37 °C, and finally $t_m = 11/4 \times t_{DIPSI2} = 19.8$ ms at 50 and 60 °C. Accurate calibration of the DIPSI2 pulses and avoiding interruption of the DIPSI2 cycle at a random point both ensure that water magnetization is correctly locked along the CP axis at the end of the CP, thus allowing its active return to the z axis to further reduce the recycle time.[29,30] To avoid intensity loss and signal broadening during ^{15}N evolution, decoupling of the ^{15}N term is performed by a second DIPSI2 train, this time centered on the water frequency, by using lower power (2.5 kHz) to reduce heating.[15,16] It is preceded by a 90° pulse at the same field strength to align water-proton magnetization along the DIPSI axis. A second proton pulse restores the water term to the z axis, where it relaxes further towards its equilibrium value during the ^{15}N-to-^{13}CO transfer period (Figure 3). The apparent relaxation rate of the amide protons being the sum of an exchange term and the true relaxation term,[31] the exchange process is already active during the N-to-CO transfer in the CP-H_NNCO sequence, thus resulting in an amide term close to equilibrium at the end of carbonyl detection. The simultaneous DIPSI2 trains on the ^{1}H and ^{15}N channels for the CP transfer can however contribute to sample heating when the duty cycle is too high. We decided to use a minimum recycle delay of 700 ms.

For direct comparison, we recorded spectra based on proton (see Figure S1) and carbon detection (Figures 1, 2, and 4) with similar total experimental times ((68 ± 4) min). The results show that proton detection remains the method of choice for slowly exchanging residues, but the signal intensity

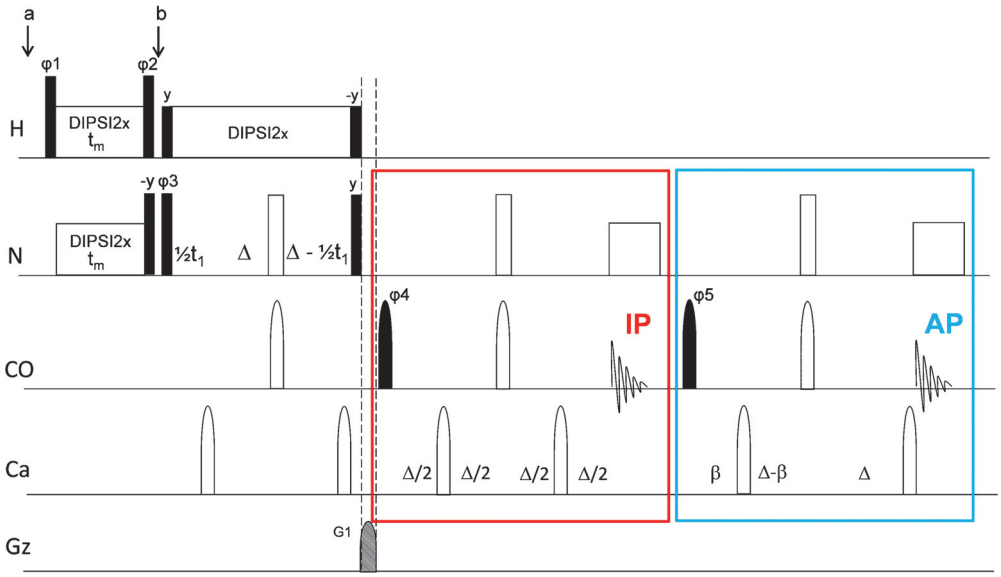

Figure 3. CP-H_NNCO pulse sequence. Filled and empty symbols indicate 90 and 180° pulses, respectively, applied along the *x* axis, unless indicated otherwise. Delays are: $4\Delta = 1/J_{NCo}$, $4\beta = 1/J_{C}\alpha_{CO}$, t_1 = F1 increment, and $t_m = J$ cross-polarization mixing time. During the J-CP DIPSI2 period, the proton radiofrequency carrier is kept in the middle of the amide region (time point a) to ensure efficient J-CP transfer. After the CP transfer, the carrier is switched to the water frequency (time point b). A pulsed field gradient G1 (1 ms, 17 Gauss cm^{-1}) is applied along the *z* axis (PFGz). Shaped carbon pulses are implemented as Gaussian cascades,[32] with Q5 shapes (400 µs) for the 90° pulses and Q3 shapes (256 µs) for the 180° pulses. ^{15}N decoupling during carbon detection uses a GARP[33] decoupling sequence (field strength of 715 Hz). Phase cycling: $\phi1 = y, -y$; $\phi2 = -y, y$; $\phi3 = x, x, -x, -x$; $\phi4 = 4(x), 4(-x)$; $\phi5 = 4(-y), 4(y)$; $\phi_{rec} = x, 2(-x), x, -x, 2(x), -x$. Quadrature detection in F1 is obtained by incrementing $\phi3$ by using the States-TPPI method.

in those experiments decreases rapidly when exchange rates increase. Experiments based on proton detection hence seem inappropriate for the study of intrinsically disordered proteins (IDPs) under physiological conditions (see Figures S1 and S2). A comparison of signal intensities in carbonyl-detection experiments as a function of temperature shows that N–CO experiments starting with amide-proton magnetization clearly exhibit superior sensitivity over the CON experiment at lower temperatures (Figure 1); however, at least the BEST-H_NNCO experiment tends to lose this advantage at higher temperatures owing to enhanced solvent exchange during the free-precession-based ^{1}H-to-^{15}N transfer and ^{15}N evolution (Figure 2). The CON experiment, although considerably less efficient at low temperatures, is rather insensitive to sample conditions in terms of the pH value and temperature,[34] thus leading to cross-over of normalized signal intensities between BEST-H_NNCO and CON experiments for temperatures between 20 and 30 °C (Figure 4). For this reason, true physiological conditions were indeed not claimed in the original study. When the initial INEPT is replaced by a J-CP transfer, intensity still drops as a function of temperature, but even for amide protons of residues characterized by rapid exchange with water, the same cross-over with the CON experiment only occurs at temperatures around 50 °C (Figure 4).

A more detailed picture of sensitivity losses as a function of temperature emerges when we compare the behavior of individual resonances with their predicted exchange rates (see Table S1) at different temperatures. At 37 °C, peak intensity in the BEST-H_NNCO experiment dropped severely for residues undergoing medium-to-fast exchange, and only peaks exhibiting very slow exchange, such as E137 (with a predicted k_{ex} value of 41 Hz at 37 °C), remained more intense than in the classical CON experiment. Under the same conditions, the CP-H_NNCO pulse sequence performed better at both temperatures (10 and 37 °C). On average, at 10 °C, signal intensity in the CP-H_NNCO spectrum was five times that of the CON experiment, and although this ratio dropped at higher temperatures, the CP-H_NNCO sequence still yielded on average 2.3 times the signal intensity of the CON experiment at 37 °C. Only at 50 °C did some peaks characterized by rapid amide-proton exchange exhibit lower sensitivity in the CP-H_NNCO spectrum than their counterparts in the CON experiment. Hence, CP transfer combined with direct CO detection constitutes an optimal strategy for the study of IDPs under physiological conditions of temperature and pH value.

To directly compare the performance of the different carbonyl-detection pulse sequences under true physiological conditions, we carried out in-cell NMR experiments at 37 °C on a slurry of *Escherichia coli* bacteria overexpressing α-synuclein. Since in-cell samples may evolve over time (degradation, leakage, pH variation),[36,37] we sought to minimize the influence of such effects on the comparison by recording one-dimensional versions of the experiments on a single sample directly one after another (total experimental time: ca. 10 min; Figure 5). Furthermore, we recorded entire two-dimensional experiments on three independent samples by changing the order of spectral recording (CP-H_NNCO, BEST-H_NNCO, and CON) in a cyclic manner (see Figure S5). We confirmed the in vitro data of Figure 4 and found that the CP-H_NNCO spectrum always exhibited the highest signal-to-noise ratio (Figure 5; see also Figure S5). In *E. coli* cells at 37 °C, the CP-H_NNCO experiment was on average 1.7 times more sensitive than the BEST-H_NNCO spectrum, and 4 times more sensitive than the CON experiment (Figure 5). We also tested the CP-H_NNCO as a nonconstant-time experiment and found only minimal intensity differences when compared to the constant-time CP-H_NNCO experiment (Figure 5). This result opens up the possibility of acquiring N–CO spectra with high resolution in the indirect dimension, as limited only by

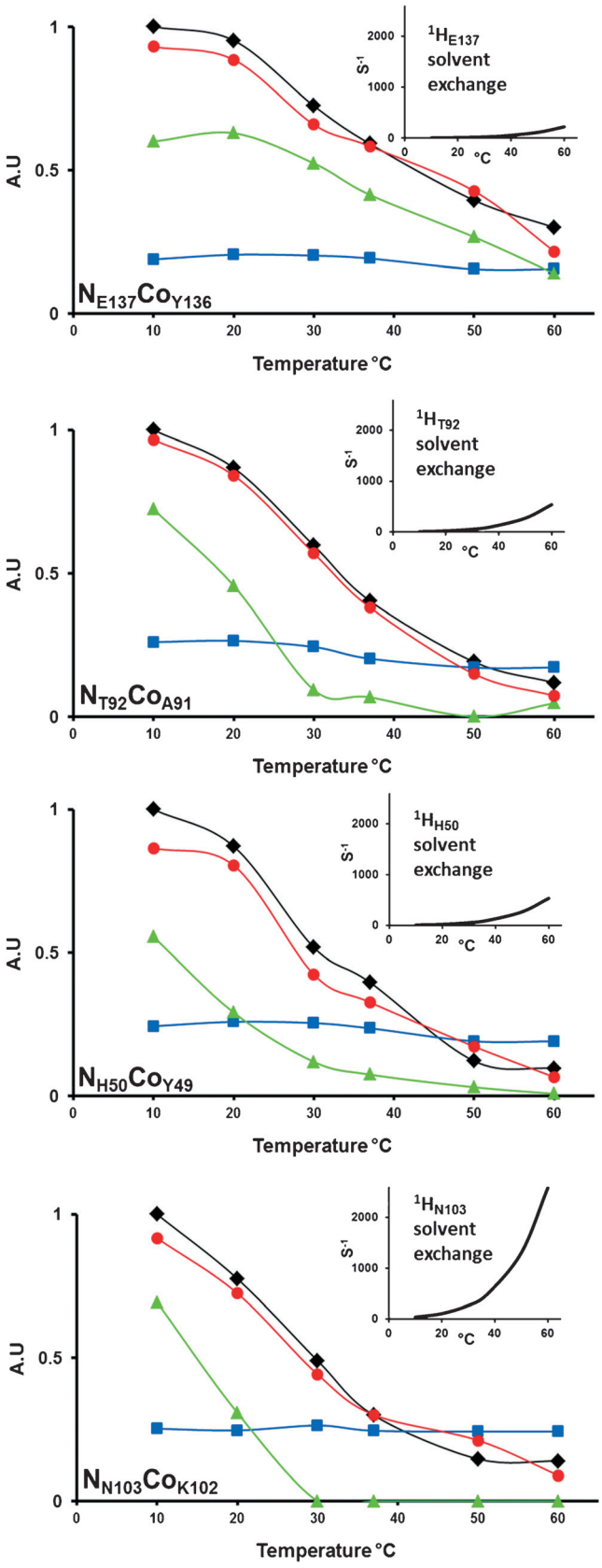

Figure 4. Comparison of normalized intensities of selected α-synuclein signals as a function of temperature in constant-time CP-H_NNCO (black diamonds), nonconstant-time CP-H_NNCO (red circles), BEST-H_NNCO (green triangles), and CON experiments (blue rectangles). The four panels correspond to residues predicted by the SPHERE server to exhibit slow (E137), intermediate (H50 and T92), or fast amide exchange (N103; see inserts and Table S1 in the Supporting Information).[35] α-Synuclein N–CO assignments were taken from the literature.[20]

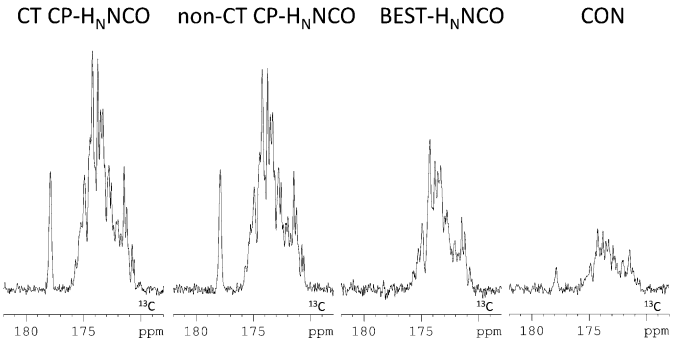

Figure 5. 1D versions of CT CP-H_NNCO (constant-time), non-CT CP-H_NNCO (nonconstant-time), BEST-H_NNCO, and CON experiments recorded on an α-synuclein in-cell sample. For experimental conditions, see the Supporting Information.

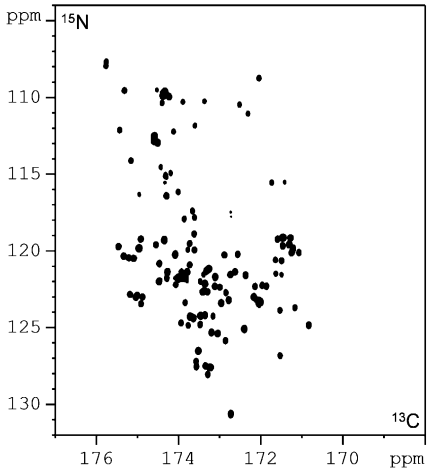

Figure 6. In-cell α-synuclein spectrum recorded at 37 °C with the nonconstant-time CP-H_NNCO pulse sequence. The sample was prepared as described in Ref. [52]. Experimental conditions are detailed in the Supporting Information.

the nitrogen T_2 relaxation rate. We thus obtained a high-quality in-cell CP-H_NNCO spectrum of α-synuclein at 37 °C and a ^1H Larmor frequency of 900 MHz with good resolution in the indirect dimension (18.5 Hz; Figure 6). Since the amide-proton–water frequency difference increases with the magnetic field, an increase in the CP field strength to 6 kHz proved important to quench the exchange contribution and avoid off-resonance effects.[38–40]

In conclusion, we highly recommend the incorporation of the J-CP block in two- and higher-dimensional carbon-detection experiments to enhance their sensitivity under physiological conditions. In-cell measurements of residual structure, dynamics, and exchange processes should strongly benefit from this approach.[41–50] Our improved CP-H_NNCO sequence opens up the possibility to perform in-cell studies of

IDPs under true mammalian physiological conditions of pH and temperature, thus offering new insight into their cellular behavior, as recently shown for α-synuclein in different neuronal cells.[51]

Acknowledgements

We thank Prof. Isabella Felli for providing the BEST-H_NNCO NMR pulse sequence and Prof. Nikolai Skrynnikov for providing the CP-HISQC NMR pulse sequence. The research leading to these results was supported by the Centre National de la Recherche Scientifique, a LABEX DISTALZ grant (Development of Innovative Strategies for a Transdisciplinary Approach to Alzheimer's Disease), and the CNRS Large Scale Facility NMR THC Fr3050. The NMR facility is funded by the European Community, the CNRS, the Région Nord-Pas de Calais (France), the University of Lille 1, and the Institut Pasteur de Lille.

Keywords: α-synuclein · carbon detection · cross-polarization · in-cell NMR spectroscopy · intrinsically disordered proteins

How to cite: *Angew. Chem. Int. Ed.* **2016**, *55*, 7418–7422
Angew. Chem. **2016**, *128*, 7544–7548

[1] P. Selenko, G. Wagner, *J. Struct. Biol.* **2007**, *158*, 244–253.
[2] A. Y. Maldonado, D. S. Burz, A. Shekhtman, *Prog. Nucl. Magn. Reson. Spectrosc.* **2011**, *59*, 197–212.
[3] R. Hänsel, L. M. Luh, I. Corbeski, L. Trantirek, V. Dötsch, *Angew. Chem. Int. Ed.* **2014**, *53*, 10300–10314; *Angew. Chem.* **2014**, *126*, 10466–10480.
[4] D. I. Freedberg, P. Selenko, *Annu. Rev. Biophys.* **2014**, *43*, 171–192.
[5] H. Tochio, S. Murayama, K. Inomata, D. Morimoto, A. Ohno, M. Shirakawa, *Yakugaku Zasshi* **2015**, *135*, 391–398.
[6] E. Luchinat, L. Banci, *J. Biol. Chem.* **2016**, *291*, 3776–3784.
[7] S. Gil, T. Hošek, Z. Solyom, R. Kümmerle, B. Brutscher, R. Pierattelli, I. C. Felli, *Angew. Chem. Int. Ed.* **2013**, *52*, 11808–11812; *Angew. Chem.* **2013**, *125*, 12024–12028.
[8] T. Yuwen, N. R. Skrynnikov, *J. Biomol. NMR* **2014**, *58*, 175–192.
[9] V. V. Krishnan, M. Rance, *J. Magn. Reson. Ser. A* **1995**, *116*, 97–106.
[10] T. Parella, *J. Biomol. NMR* **2004**, *29*, 37–55.
[11] T. Parella, *J. Magn. Reson.* **2004**, *167*, 266–272.
[12] P. Nolis, T. Parella, *Curr. Anal. Chem.* **2007**, *3*, 47–68.
[13] A. G. Palmer, J. Cavanagh, P. E. Wright, M. Rance, *J. Magn. Reson.* **1991**, *93*, 151–170.
[14] P. Schanda, H. Van Melckebeke, B. Brutscher, *J. Am. Chem. Soc.* **2006**, *128*, 9042–9043.
[15] A. Bax, M. Ikura, L. E. Kay, D. A. Torchia, R. Tschudin, *J. Magn. Reson.* **1990**, *86*, 304–318.
[16] J. Iwahara, Y.-S. Jung, G. M. Clore, *J. Am. Chem. Soc.* **2007**, *129*, 2971–2980.
[17] J. Lopez, P. Ahuja, M. Gerard, J.-M. Wieruszeski, G. Lippens, *J. Magn. Reson.* **2013**, *236*, 1–6.
[18] M. Kostic, S. S. Pochapsky, T. C. Pochapsky, *J. Am. Chem. Soc.* **2002**, *124*, 9054–9055.
[19] W. Bermel, I. Bertini, L. Duma, I. C. Felli, L. Emsley, R. Pierattelli, P. R. Vasos, *Angew. Chem. Int. Ed.* **2005**, *44*, 3089–3092; *Angew. Chem.* **2005**, *117*, 3149–3152.
[20] W. Bermel, I. Bertini, I. C. Felli, Y.-M. Lee, C. Luchinat, R. Pierattelli, *J. Am. Chem. Soc.* **2006**, *128*, 3918–3919.
[21] B. O'Hare, A. J. Benesi, S. A. Showalter, *J. Magn. Reson.* **2009**, *200*, 354–358.
[22] W. Bermel, I. Bertini, J. Chill, I. C. Felli, N. Haba, Vasantha Kumar M. V., R. Pierattelli, *ChemBioChem* **2012**, *13*, 2425–2432.
[23] I. C. Felli, R. Pierattelli, *J. Magn. Reson.* **2014**, *241*, 115–125.
[24] W. Bermel, M. Bruix, I. C. Felli, Vasantha Kumar M. V., R. Pierattelli, S. Serrano, *J. Biomol. NMR* **2013**, *55*, 231–237.
[25] W. Bermel, I. Bertini, V. Csizmok, I. C. Felli, R. Pierattelli, P. Tompa, *J. Magn. Reson.* **2009**, *198*, 275–281.
[26] W. Bermel, I. Bertini, I. C. Felli, R. Pierattelli, *J. Am. Chem. Soc.* **2009**, *131*, 15339–15345.
[27] A. J. Shaka, C. J. Lee, A. Pines, *J. Magn. Reson.* **1988**, *77*, 274–293.
[28] J. Cavanagh, M. Rance, *J. Magn. Reson.* **1992**, *96*, 670–678.
[29] M. Piotto, V. Saudek, V. Sklenár, *J. Biomol. NMR* **1992**, *2*, 661–665.
[30] C. Dhalluin, J.-M. Wieruszeski, G. Lippens, *J. Magn. Reson. Ser. B* **1996**, *111*, 168–170.
[31] P. R. Rosevear, D. C. Fry, A. S. Mildvan, *J. Magn. Reson.* **1985**, *61*, 102–115.
[32] L. Emsley, G. Bodenhausen, *Chem. Phys. Lett.* **1990**, *165*, 469–476.
[33] A. J. Shaka, P. B. Barker, R. Freeman, *J. Magn. Reson.* **1985**, *64*, 547–552.
[34] S.-T. D. Hsu, C. W. Bertoncini, C. M. Dobson, *J. Am. Chem. Soc.* **2009**, *131*, 7222–7223.
[35] Y. Bai, J. S. Milne, L. Mayne, S. W. Englander, *Proteins Struct. Funct. Genet.* **1993**, *17*, 75–86.
[36] J. L. Slonczewski, B. P. Rosen, J. R. Alger, R. M. Macnab, *Proc. Natl. Acad. Sci. USA* **1981**, *78*, 6271–6275.
[37] J. C. Wilks, J. L. Slonczewski, *J. Bacteriol.* **2007**, *189*, 5601–5607.
[38] P. Lundström, M. Akke, *J. Biomol. NMR* **2005**, *32*, 163–173.
[39] D. F. Hansen, L. E. Kay, *J. Biomol. NMR* **2007**, *37*, 245–255.
[40] J. T. Spear, J. C. Gore, *NMR Biomed.,* DOI: 10.1002/nbm.3490.
[41] J.-F. Bodart, J.-M. Wieruszeski, L. Amniai, A. Leroy, I. Landrieu, A. Rousseau-Lescuyer, J.-P. Vilain, G. Lippens, *J. Magn. Reson.* **2008**, *192*, 252–257.
[42] G. Lippens, I. Landrieu, X. Hanoulle, *Chem. Biol.* **2008**, *15*, 311–312.
[43] C. A. Waudby, M. D. Mantle, L. D. Cabrita, L. F. Gladden, C. M. Dobson, J. Christodoulou, *J. Am. Chem. Soc.* **2012**, *134*, 11312–11315.
[44] A. Binolfi, F.-X. Theillet, P. Selenko, *Biochem. Soc. Trans.* **2012**, *40*, 950–954.
[45] C. Li, M. Liu, *FEBS Lett.* **2013**, *587*, 1008–1011.
[46] T. K. S. Kumar, R. Thurman, S. Jayanthi, *J. Anal. Bioanal. Tech.* **2013**, *4*, e112.
[47] C. A. Waudby, C. Camilloni, A. W. P. Fitzpatrick, L. D. Cabrita, C. M. Dobson, M. Vendruscolo, J. Christodoulou, *PloS One* **2013**, *8*, e72286.
[48] S. Majumder, C. M. DeMott, D. S. Burz, A. Shekhtman, *ChemBioChem* **2014**, *15*, 929–933.
[49] J. Danielsson, X. Mu, L. Lang, H. Wang, A. Binolfi, F.-X. Theillet, B. Bekei, D. T. Logan, P. Selenko, H. Wennerström, M. Oliveberg, *Proc. Natl. Acad. Sci. USA* **2015**, *112*, 12402–12407.
[50] A. E. Smith, Z. Zhang, G. J. Pielak, C. Li, *Curr. Opin. Struct. Biol.* **2015**, *30*, 7–16.
[51] F.-X. Theillet, A. Binolfi, B. Bekei, A. Martorana, H. M. Rose, M. Stuiver, S. Verzini, D. Lorenz, M. van Rossum, D. Goldfarb, P. Selenko, *Nature* **2016**, *530*, 45–50.
[52] I. C. Felli, L. Gonnelli, R. Pierattelli, *Nat. Protoc.* **2014**, *9*, 2005–2016.

Received: February 22, 2016
Revised: March 28, 2016
Published online: May 9, 2016

